Predicting Frictional Properties of Graphene Kirigami Using Molecular Dynamics and Neural Networks

Designs for a negative friction coefficient

Mikkel Metzsch Jensen

University of Oslo

Juni 02, 2023

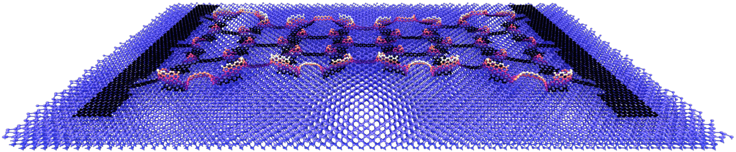

Outline

Thesis overview

1. **Sheet modification**: Alter a graphene sheet using atomic scale cuts and stretching
2. **Forward simulation**: Calculate the frictional properties of the sheet using MD simulations
3. **Accelerated search**: Use machine learning to replace the MD simulations and perform an accelerated search for new designs

Main research question

Can we control the friction of a nanoscale Kirigami sheet with pattern design and straining of the sheet?

- Kirigami: Variation of origami with cuts permitted
- Desgins: Macroscale $\rightarrow$ nanoscale

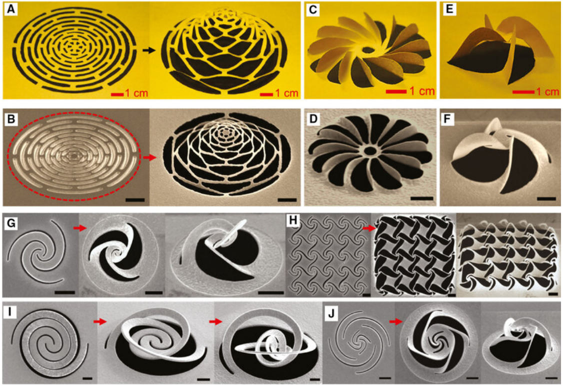

Figure: Example of macroscale Kirigami designs implemented on a microscale using a focused ion beam. Black scale bars: 1 μm. Reproduced from [1].

- Hanakata et al. [2, 3] found out-of-plane buckling with Kirigami designs
- Surface properties are predicted to be important for friction properties
  - Asperity theory: Contact area
  - Frenkel–Kontorova models: Commensurability

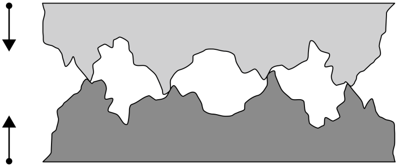

(a) Small load.

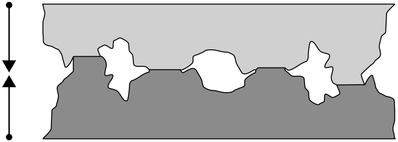

(b) High load.

Figure: Qualitatively illustration of the microscopic asperity deformation under increasing load. Reproduced from [4].

Motivation

Contact area and commensurability

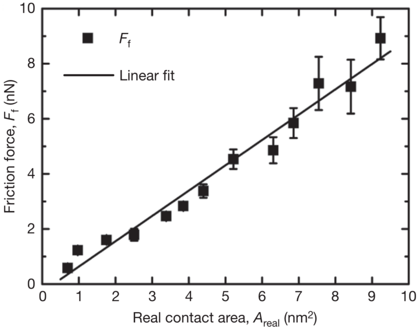

(a) Numerical MD results using an amorphous carbon tip and a diamond sample. Reproduced from [5] with permission from Springer Nature.

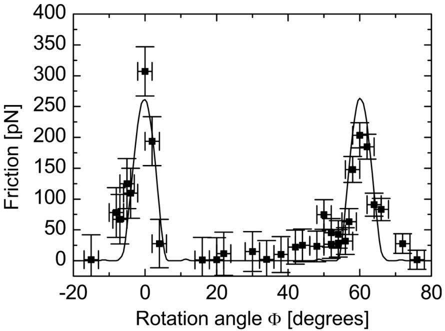

(b) Experimental results of a graphene sheet sliding on graphite. Adapted from [6], reproduced from [7] with permission from the American Physical Society.

Creating a graphene Kirigami system

System setup

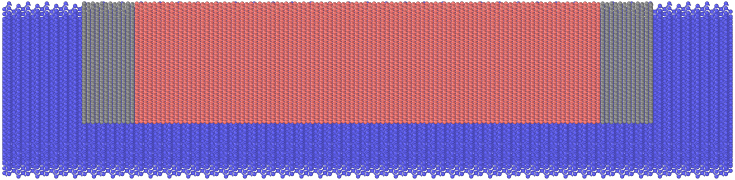

Figure: System of interest: Graphene sheet on a silicon substrate. Blue: Substrate, Red: Inner sheet, Grey: Pull blocks.

System setup

System size

$$\text{Atoms} \sim 60,000$$

$$\text{Sheet} \sim 130 \times 165\,\text{Å}$$

Regions

- Red: *NVE*
- Green: Thermostat *NVT*
- Blue: Rigid

(a) Side view.

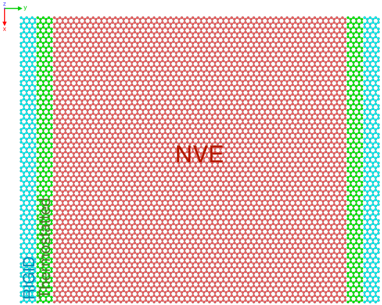

(b) Top view.

Sheet Kirigami

Indexing

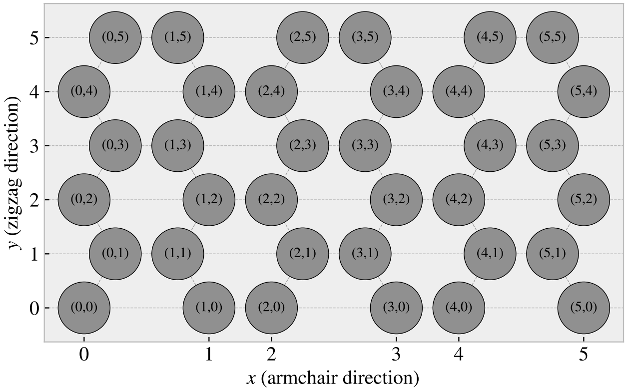

Figure: Graphene atom site indexing.

Sheet Kirigami
Indexing

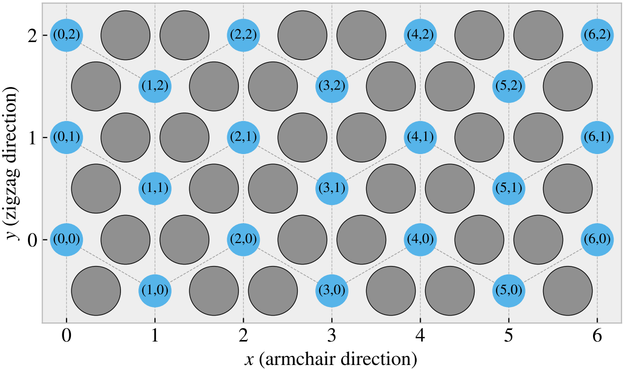

Figure: Graphene *center element* indexing.

Sheet Kirigami

Macroscale inspiration

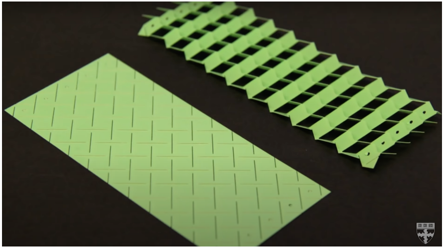

(a) Tetrahedron: Alternating perpendicular cuts producing a tetrahedron-shaped surface buckling when stretched. Reproduced from [8].

(b) Honeycomb: Scotch^{TM} Cushion Lock^{TM} [9] producing a honeycomb-shaped surface buckling when stretched. Reproduced from [9].

Figure: Macroscale kirigami cut patterns used as inspiration for the nanoscale implementation.

Sheet Kirigami

Tetrahedron patterns

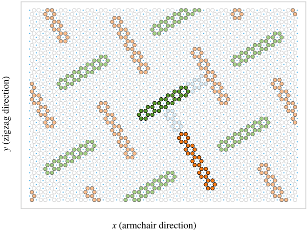

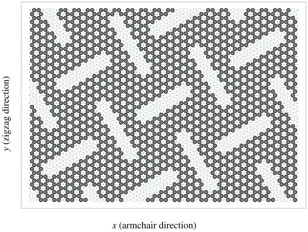

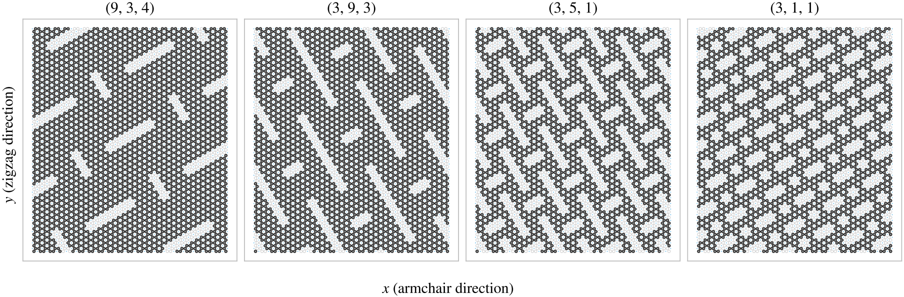

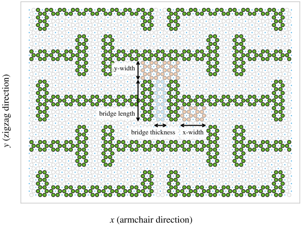

y-width
bridge length
bridge thickness
x-width
y (zigzag direction)
x (armchair direction)

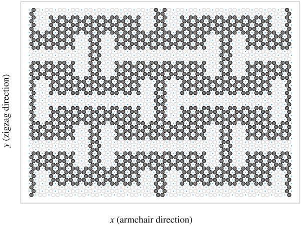

y (zigzag direction)
x (armchair direction)

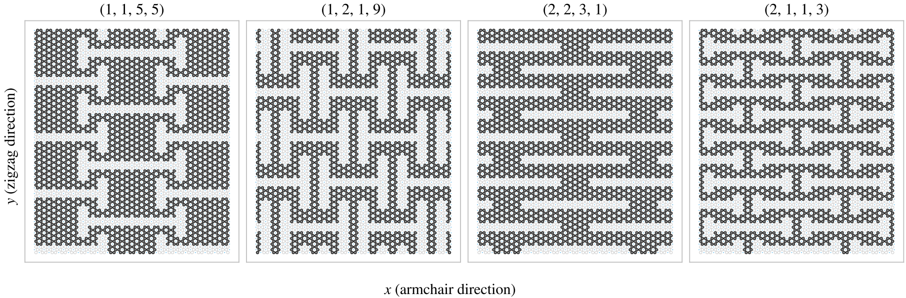

(1, 1, 5, 5)
(1, 2, 1, 9)
(2, 2, 3, 1)
(2, 1, 1, 3)
y (zigzag direction)
x (armchair direction)

Sheet Kirigami
Random walk patterns

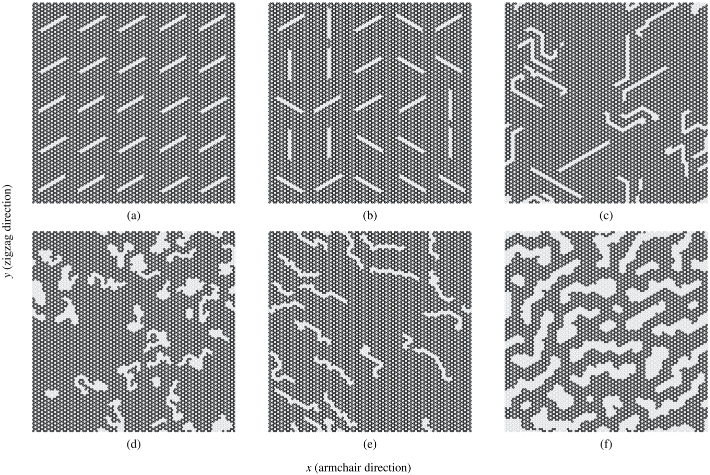

Molecular Dynamics (MD)

Newtons equations (NVE)

$$m_i \frac{d^2 \mathrm{r}_i}{dt^2} = \mathrm{F}_i = -\nabla U_i,$$

Introducing temperature (NVT) with the Langevin equation

$$m_i \frac{d^2 \mathrm{r}_i}{dt^2} = \underbrace{-\nabla U_i}_{F_i} \underbrace{-\alpha \mathrm{v}_i}_{\text{Drag}} + \underbrace{\mathrm{R}_i}_{\text{Fluctuation}},$$

$$\langle R \rangle = 0, \qquad \langle R^2 \rangle = 2\alpha k_B T.$$

Outline

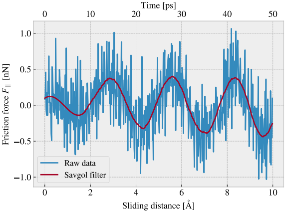

(a) $K = \infty$, $v = 20\ \frac{\text{m}}{\text{s}}$ (10 Å sliding).

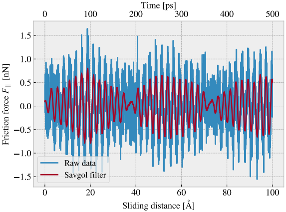

(b) $K = \infty$, $v = 20\ \frac{\text{m}}{\text{s}}$ (100 Å sliding).

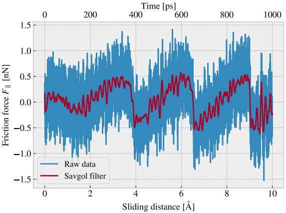

(c) $K = 10\ \frac{\text{N}}{\text{m}}$, $v = 1\ \frac{\text{m}}{\text{s}}$ (10 Å sliding).

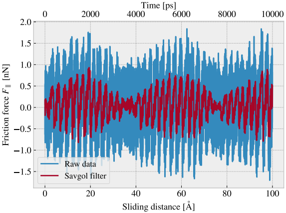

(d) $K = 10\ \frac{\text{N}}{\text{m}}$, $v = 1\ \frac{\text{m}}{\text{s}}$ (100 Å sliding).

Figure: Force traces of the friction force component $F_\parallel$ parallel to the sliding direction acting from the substrate on the full sheet. The red line represents a Savgol filter

Pilot study
Out-of-plane buckling

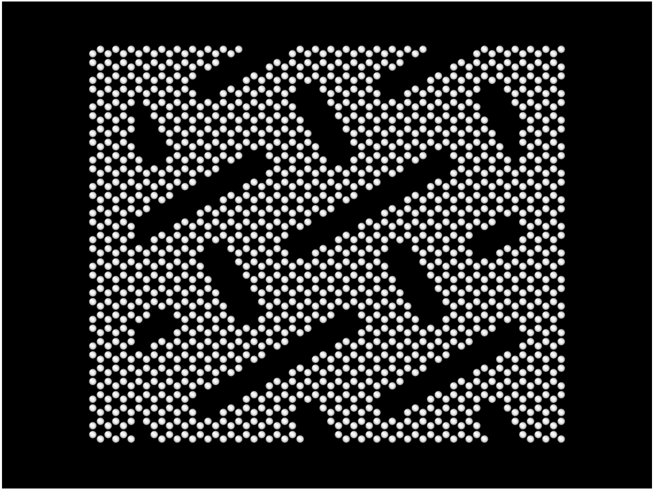

Figure: Kirigami sheet stretch in vacuum. Small tetrahedron pattern.

Pilot study
Out-of-plane buckling

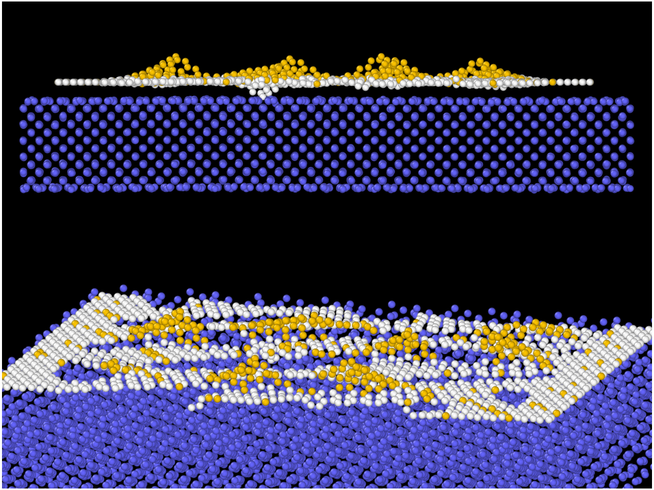

Figure: Kirigami stretch in contact with Si-substrate.

Pilot study

Out-of-plane buckling

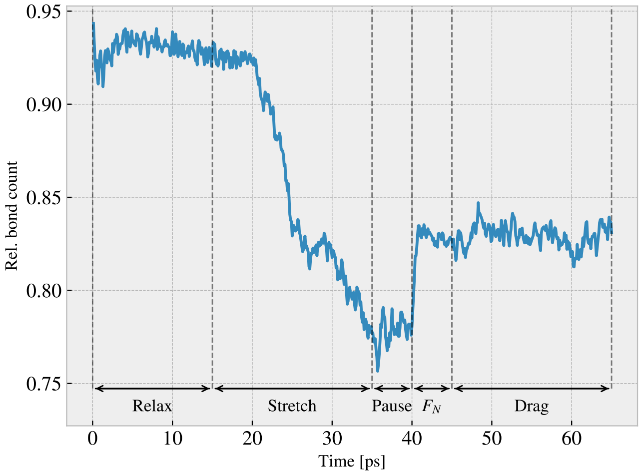

Figure: Contact area approximation: Number of C-Si bonds within a threshold distance of 110% the LJ interaction equilibrium distance.

Pilot study

Friction-strain profiles

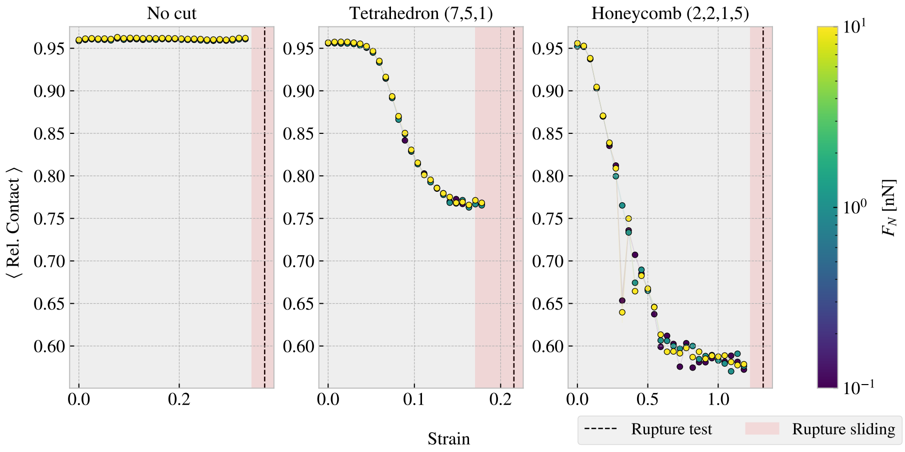

Pilot study
Friction-strain profiles

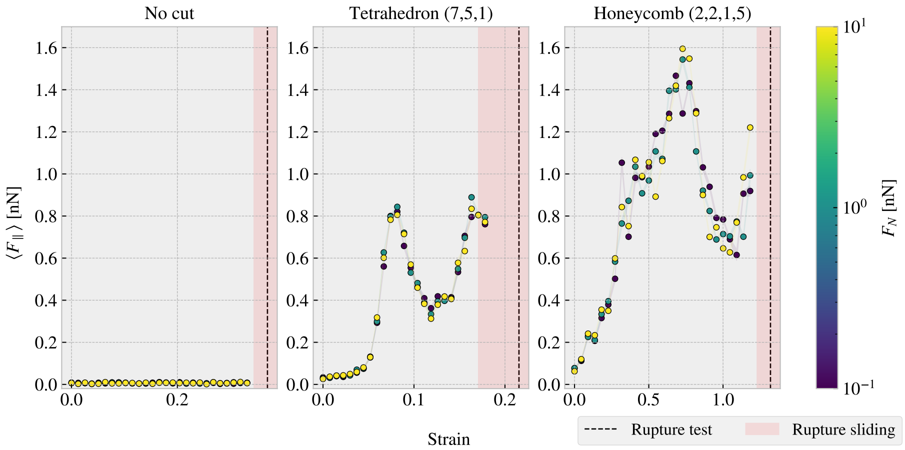

Pilot study

Negative friction coefficient

Load to sheet tension coupling

$$F_t = TF_N, \qquad T = 6$$

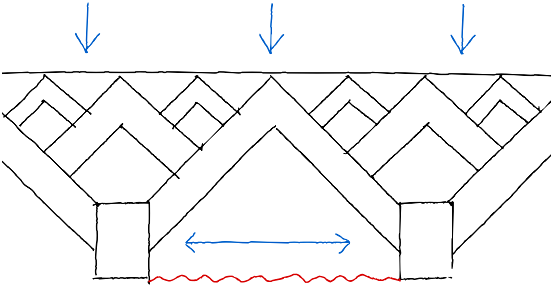

Pilot study

Negative friction coefficient

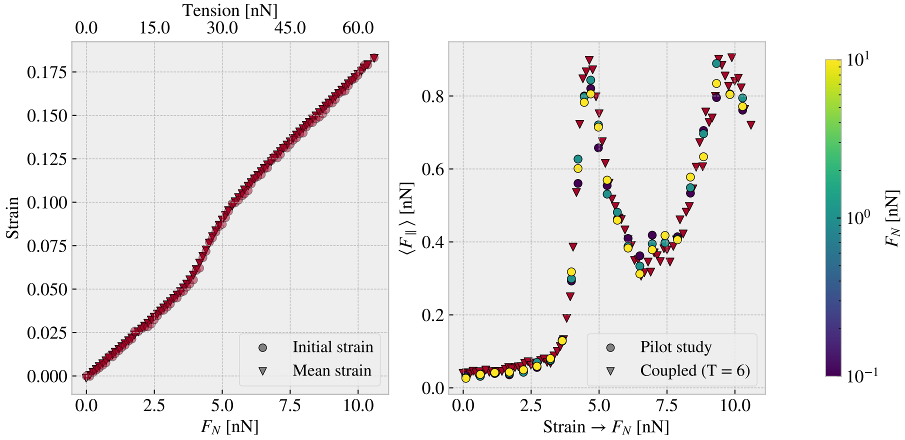

Figure: Tetrahedron $(7, 5, 1)$

Pilot study

Negative friction coefficient

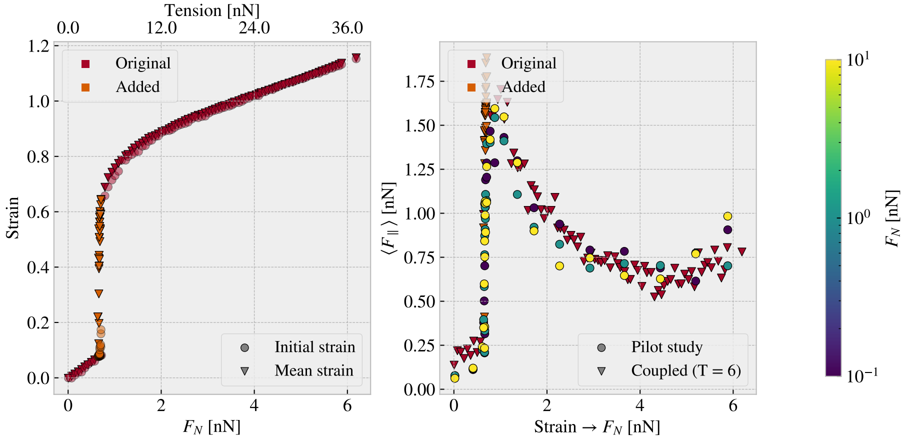

Figure: Honeycomb $(2, 2, 1, 5)$

Pilot study

Negative friction coefficient

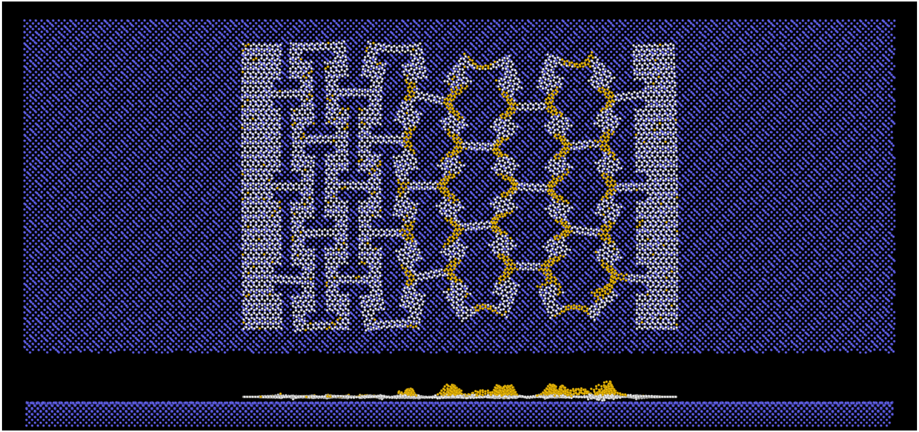

Figure: Honeycomb $(2, 2, 1, 5)$ stretch.

Outline

Kirigami configuration search
Dataset

Table: Summary of the generated data points in the dataset.

Type	**Configurations**	**Submitted**	**Final**	**Ruptures**
Pilot study	3	270	261	25 (9.58 %)
Tetrahedron	68	3060	3015	391 (12.97 %)
Honeycomb	45	2025	1983	80 (4.03 %)
Random walk	100	4500	4401	622 (14.13 %)
Total	214 (216)	9855	9660	1118 (11.57 %)

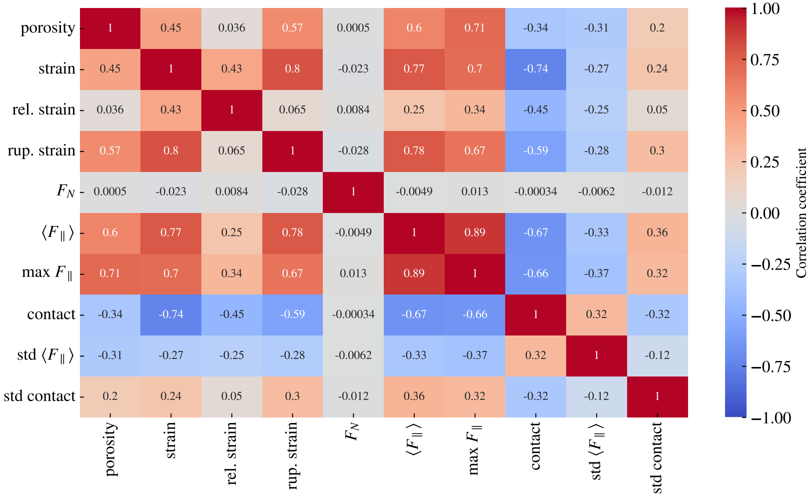

Figure: Pearson product-moment correlation coefficients.

Properties of interest

$$\min F_{\text{fric}}, \qquad \max F_{\text{fric}}, \qquad \max \Delta F_{\text{fric}}, \qquad \max \text{drop}.$$

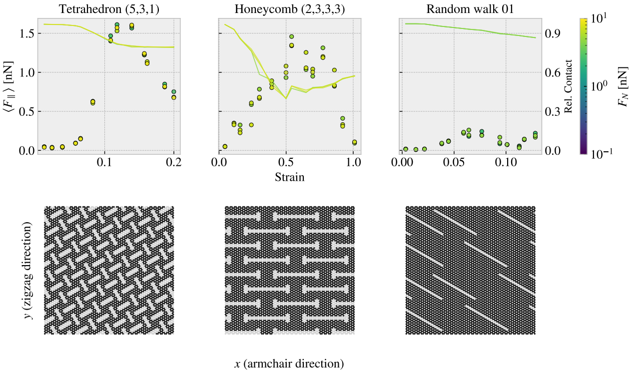

Figure: Max drop property. Best candidates in the dataset.

Kirigami configuration search
ML

- Convolutional neural network
- Input: Configuration, strain and load
- Output: Mean friction, maximum friction, contact area, porosity, rupture, rupture strain

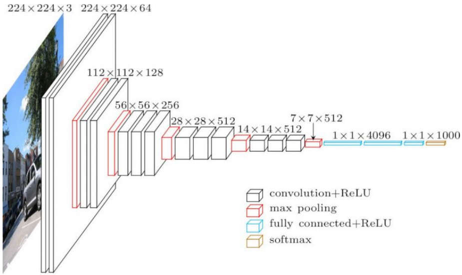

Figure: Illustration of the convolutional network architecture for the VGGNet-16 network. Reproduced from [10].

Table: Evaluation of the final model performance.

	R^2 $[10^2]$			Abs. $[10^2]$	Rel. $[10^2]$	Acc. $[10^2]$
	Mean F_f	Max F_f	Contact	Porosity	Rup. Strain	Rupture
Validation	98.067	93.558	94.598	2.325	12.958	96.102
Tetrahedron	88.662	85.836	64.683	1.207	5.880	99.762
Honeycomb	96.627	89.696	97.171	1.040	1.483	99.111

Kirigami configuration search
ML

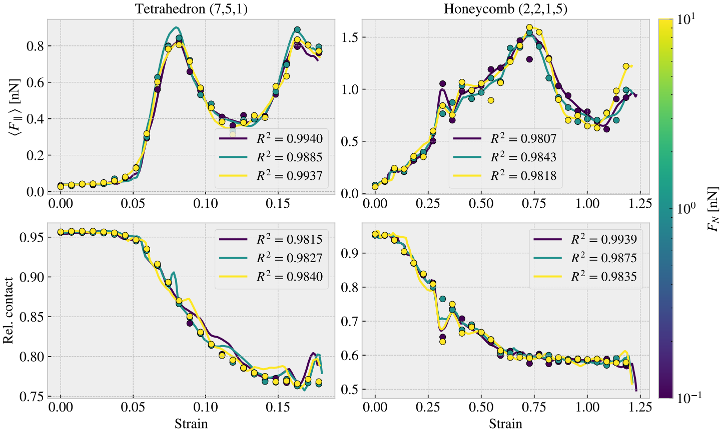

Figure: Visual evaluation of the final model predictions on the Tetrahedron $(7, 5, 1)$ and Honeycomb $(2, 2, 1, 5)$ used in the pilot study.

We generate an extended dataset.

- Tetrahedron: 1.35×10^5 configurations
- Honeycomb: 2.025×10^6 configurations
- Random walk: 10^4 configurations

Kirigami configuration search

Accelerated search

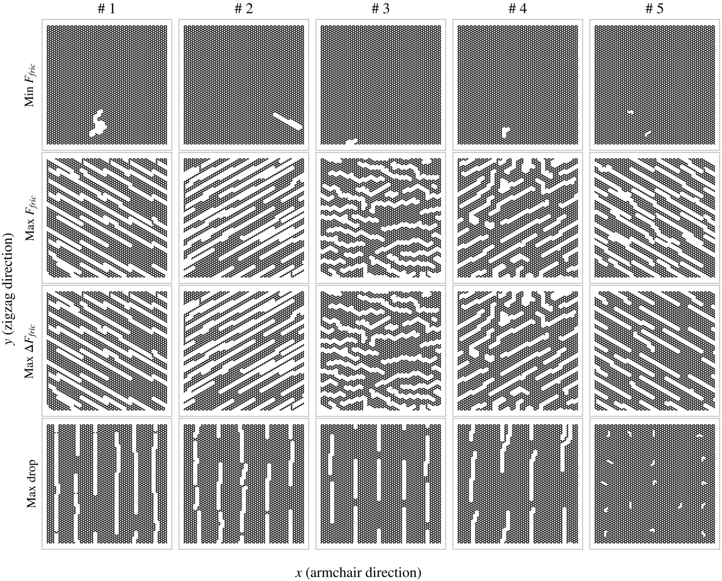

Kirigami configuration search

Accelerated search

Translational variance

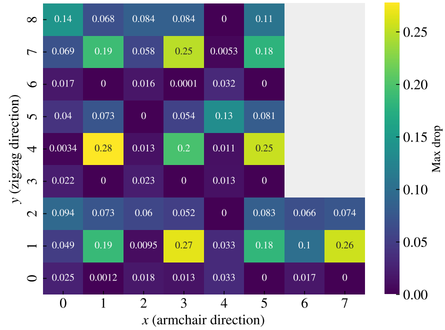

(a) Tetrahedron $(1, 7, 1)$ (60). Std $= 0.08$, Rel. Std $= 1.13$

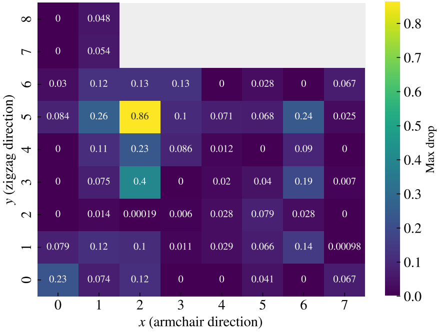

(b) Tetrahedron $(5, 3, 1)$ (60). Std $= 0.13$, Rel. Std $= 1.61$

Figure: Prediction of the max drop property for selected patterns using the machine learning model for all unique reference positions.

Genetic algorithm based on Markov chain probability.

1. Rank configurations by fitness score.
2. Assign a mutation probability based on the ranking.
3. Calculate target states from the best candidates.
4. Mutate and repeat.

Poor convergence on the mac drop property optimization

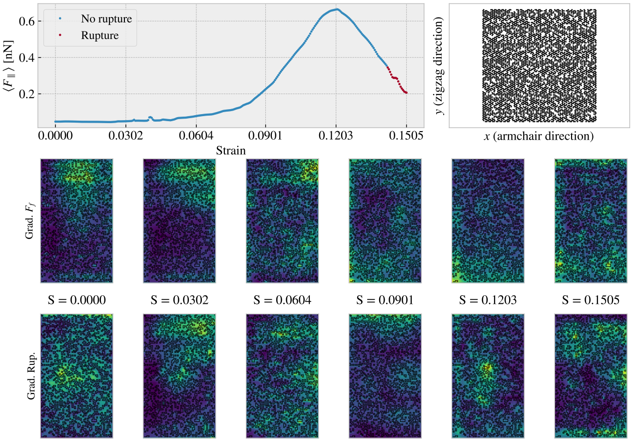

Figure: Genetic algorithm suggestion from a mixed porosity start. Top: Friction-strain curve and configuration. Bottom: Grad-CAM analysis

Grad-CAM

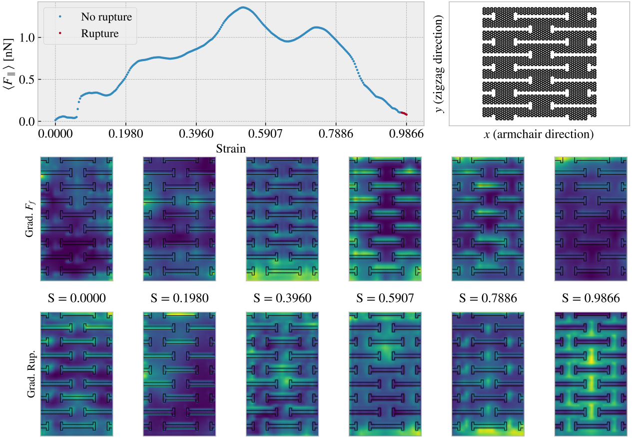

Figure: Honeycomb $(3, 3, 5, 3)$, ref $= (12, 0)$.

Outline

Summary and outlook

Key findings

- Non-monotonous relationship between friction and strain
- Coupled system can be exploited to achieve a negative friction coefficient
- Machine learning is feasible but more data is needed

Further studies:

- Investigation of the underlying mechanism
  - Commensurability hypothesis can be investigated by varying scan angle
- Friction-strain relationship at different physical conditions: temperature, sliding speed, spring stiffness.
- Edge and thermostat effects.
- Improve dataset with active learning

References I

[1] J. Li and L. Zhiguang, "Focused-ion-beam-based nano-kirigami: from art to photonics", Nanophotonics **7**, 10.1515/nanoph-2018-0117 (2018).

[2] P. Z. Hanakata, E. D. Cubuk, D. K. Campbell, and H. S. Park, "Accelerated search and design of stretchable graphene kirigami using machine learning", Phys. Rev. Lett. **121**, 255304 (2018).

[3] P. Z. Hanakata, E. D. Cubuk, D. K. Campbell, and H. S. Park, "Forward and inverse design of kirigami via supervised autoencoder", Phys. Rev. Res. **2**, 042006 (2020).

[4] W. Commons, *File:asperities.svg — wikimedia commons, the free media repository*, (2023) https://commons.wikimedia.org/w/index.php?title=File:Asperities.svg&oldid=659167170 (visited on 02/03/2023).

[5] Y. Mo, K. T. Turner, and I. Szlufarska, "Friction laws at the nanoscale", Nature **457**, 1116–1119 (2009).

References II

[6] M. Dienwiebel, N. Pradeep, G. S. Verhoeven, H. W. Zandbergen, and J. W. Frenken, "Model experiments of superlubricity of graphite", Surface Science **576**, 197–211 (2005).

[7] A. Vanossi, N. Manini, M. Urbakh, S. Zapperi, and E. Tosatti, "Modeling friction: from nanoscale to mesoscale", Reviews of Modern Physics **85**, 529–552 (2013).

[8] L. Burrows, *New pop-up strategy inspired by cuts, not folds*, (Feb. 24, 2017) https://seas.harvard.edu/news/2017/02/new-pop-strategy-inspired-cuts-not-folds.

[9] *Scotch cushion lock protective wrap*, https://www.scotchbrand.com/3M/en_US/scotch-brand/products/catalog/~/Scotch-Cushion-Lock-Protective-Wrap/?N=4335+3288092498+3294529207&rt=rud.

[10] Neurohive, *VGG16 — Convolutional Network for Classification and Detection*, (2018) https://neurohive.io/en/popular-networks/vgg16/ (visited on 05/07/2023).